Fish and Shellfish Immunology 94 (2019) 852–860

Contents lists available at ScienceDirect

Fish and Shellfish Immunology

journal homepage: www.elsevier.com/locate/fsi

Full length article

*Sp*BAG1 promotes the WSSV infection by inhibiting apoptosis in mud crab (*Scylla paramamosain*)

Xiaomeng Ma[a,b,c,1], Xixiang Tang[d,1], Shanmeng Lin[a,b,c], Yi Gong[a,b,c], Ngoc Tuan Tran[a,b,c], Huaiping Zheng[a,b,c], Hongyu Ma[a,b,c], Jude Juventus Aweya[a,b,c], Yueling Zhang[a,b,c], Shengkang Li[a,b,c,*]

[a] Guangdong Provincial Key Laboratory of Marine Biology, Shantou University, Shantou, 515063, China
[b] Marine Biology Institute, Shantou University, Shantou, 515063, China
[c] STU-UMT Joint Shellfish Research Laboratory, Shantou University, Shantou, 515063, China
[d] Key Laboratory of Marine Genetic Resources, Third Institute of Oceanography, Ministry of Natural Resources, Xiamen, 361005, China

ARTICLE INFO

Keywords:
Mud crab
WSSV
*Sp*BAG1
Apoptosis

ABSTRACT

Bcl-2 associated athanogene-1 (BAG1) is involved in various signalling pathways including apoptosis, cell proliferation, gene transcriptional regulation and signal transduction in animals. However the functions of BAG1 during the antiviral response of mud crab *Scylla paramamosain* is still unclear. In this study, the mud crab BAG1 (*Sp*BAG1) was characterized to consist of 1761 nucleotides, containing an opening frame of 630bp encoding 209 amino acids with an ubiquitin domain and a BAG1 domain. *Sp*BAG1 was found to be significantly up-regulated at 6 h–24 h, but down-regulated from 48 h–72 h in the hemocytes of mud crab after challenge with white spot syndrome virus (WSSV). RNAi knock-down of *Sp*BAG1 significantly reduced the copies of WSSV and increased the apoptotic rate in mud crabs. The finding from this study suggested that *Sp*BAG1 could promote the WSSV infection by inhibiting apoptosis in mud crab. Therefore, to the best of our knowledge, this is the first study demonstrating the role of *Sp*BAG1 as a novel apoptosis inhibitor to promote virus infection in mud crab.

1. Introduction

Mud crab (*S. paramamosain*), a commercially important crustacean species, is widely distributed along the coastal line of southern China [1]. The rapid expansion in mariculture industry and popularization of intensive aquaculture, lead to the impacts on the cultured species, including mud crab. Several pathogens, such as bacteria, parasites, and virus, have been reported to be important as the main causes of disease outbreak in aquatic animals. Of them, the white spot syndrome virus (WSSV) was one of the most important viral pathogens in crab aquaculture. WSSV is mainly transmitted from shrimp to crabs in the process of fish-shrimp-crab mixed culture [2]. At present, lots of WSSV proteins have been confirmed to be involved in WSSV infection, DNA binding, nuclear localization, viral envelope and nuclear capsid composition [3–6]. Although mud crab *S. paramamosain* has been artificial cultured for a long time, little knowledge is available on how crabs respond to viral infection.

Like other invertebrates, crabs lack acquired immune system and relies mainly on innate immunity to resist the invasion of pathogenic microorganisms, including recognition, prophenoloxidase (proPO)-activating system, phagocytosis, encapsulation, nodule formation, apoptosis, the microbicidal activity of cytotoxic reactive oxygen compounds and antimicrobial peptides (AMPs) [7]. Apoptosis, also named programmed cell death, whose initial description was based on typical morphological features such as shrunken organelles, condensed chromatin, formation of apoptotic bodies and absence of inflammation in the adjacent areas [8,9]. Apoptosis is essential in both the development and homeostasis of multicellular organisms and many of its components are remarkably conserved from worms to humans [10]. Regarding the immune response, apoptosis has been described as an effector mechanism in invertebrates [11,12], and proposed as the main anti-viral mechanism in invertebrates [13]. Up to now, many apoptosis-related genes have been reported in the vertebrates, such as Bcl-2, myc, p53 and BAG1, but few in invertebrates.

The first BAG1 gene was identified when screening for Bcl-2 binding proteins, BAG1 is composed of BAG domain (110–124 amino acids), which serves as the major function domain of BAG1 protein, responsible for the anti-apoptotic activity of BAG family proteins [14]. It

* Corresponding author. Guangdong Provincial Key Laboratory of Marine Biology, Shantou University, Shantou, 515063, China.
E-mail address: lisk@stu.edu.cn (S. Li).
[1] These authors contributed equally to this paper.

https://doi.org/10.1016/j.fsi.2019.10.013
Received 20 April 2019; Received in revised form 27 September 2019; Accepted 6 October 2019
Available online 07 October 2019
1050-4648/

has been reported that BAG1 could bind to Raf-1 serine/threonine kinase or Hsc70/Hsp70 [15,16], and promote cell proliferation by binding and stimulating of Raf-1 activity. Activated Raf-1 can activate its downstream extracellular signal-related kinase (ERK) activity and promote cell proliferation [17]. In addition, upon the stimulation of external factors (i.e. increased expression of Hsp70), the cells can compete with Raf-1 to bind to BAG1 and then, significantly weakens the Raf-1 signalling and inhibit subsequent biological events (including promoting DNA synthesis and cell cycle arrest effects) [18]. As an anti-apoptotic gene, BAG1 has been exclusively studied in a variety of cancer cells in higher animals. However, the roles of BAG-1 in invertebrates, especially in mud crab still need to be further explored.

In an attempt to explore the role of BAG1 in mud crab, the involvement of BAG1 in the regulation of apoptosis and the antiviral response was characterized in this study. The results indicated that *Sp*BAG1 could promote the invasion of the virus through inhibiting the apoptosis of the hemocytes in mud crab.

2. Materials and methods

2.1. Experimental animals and WSSV challenge test

A total of 48 healthy mud crab (50–100 g) were purchased from a crab farm in Niutianyang (Shantou, Guangdong, China), and acclimatized in laboratory tanks for one week before further processing. During the acclimatization period, the salinity (10‰) and temperature (25 °C) were maintained. After acclimatization, tissues (stomach, intestines, hepatopancreas, muscle, epidermis, hemocytes, gills, and heart) from three healthy crabs were collected and then used for investigation of the tissue distribution of the *Sp*BAG1. For challenge experiment, a volume of 200 μL of white spot syndrome virus (WSSV) (1×10^7 *cfu* mL^{-1}) were injected into the base of the fourth leg of each crab. For blank control, a similar volume of PBS was used. The experiments were conducted under the laboratory conditions (salinity of 10‰ and temperature of 25 °C) for three days.

2.2. Sample collection and RNA isolation

At 0, 6, 12, 24, 48, and 72 h post injection (hpi), the hemolymph from three crabs per group was collected mixed with an equal volume of anticoagulant solution (1.32% sodium citrate, 0.48% citric acid, and 1.47% glucose), and then centrifuged at 800 ×*g* for 20 min at 4 °C to separate the hemocytes, which was then used for RNA extraction using a test kit (TRIzol® Reagent, Ambion, USA). Furthermore, eight tissues (including stomach, intestine, hepatopancreas, muscle, epidermis, hemocytes, gills, and heart) of three mud crab were collected, rinsed with 0.1% diethylpyrocarbonate (DEPC)-treated water), immediately dipped into liquid nitrogen, and then stored in −80 °C until use for total RNA extraction using a Total RNA Rapid Extraction Kit (Feijie, Shanghai, China). The total RNA extraction was performed following the manufacturer's protocols The quality and quantity of extracted RNA were evaluated using 1.0% (w/v) agarose-gel electrophoresis and a Nanodrop® ND-1000 spectrophotometer(LabTech, Holliston, MA) at absorbance 260 nm/280 nm (A260/280). Total RNAs were used as templates to synthesize the first-strand cDNA using the PrimeScriptRT reagent Kit (TaKaRa, Dalian, China) according to the manufacturer's protocol.

2.3. Gene cloning and sequence analysis

The cDNA sequence, containing a full ORF of *Sp*BAG1, was obtained from our previous high-throughput transcriptome data. To verify the nucleotide sequence and amplify the *Sp*BAG1 3′-ends, the total RNA from hemocytes was reversely transcribed to the first-strand cDNA using M-MLV First-Strand cDNA Synthesis Kit (Invitrogen, USA). The cDNA was diluted 1/10 and used as templates for PCR. Special primers ORFF and ORFR (Table 1) were used for the amplification of the ORF. The PCR procedure was as follows: 94 °C for 5 min, 30 cycles of 94 °C for 30 s, 58 °C for 30 s, 72 °C for 80 s; and a final extension at 72 °C for 10 min. The amplified nucleotide sequence was ligated into pMD®19-T vector (TaKaRa, Dalian, China) and then transformed into *Escherichia coli*. Positive recombinant clones were identified by PCR screening with M13R and M13F primers and sequenced by a commercial company (BGI, Shenzhen, China).

The sequence homology analysis between *Sp*BAG1 and those of other species were analyzed using Basic Local Alignment Search Tool (https://blast.ncbi.nlm.nih.gov). The translation and prediction for the molecular mass and isoelectric point of the deduced amino acid sequence were performed employing ExPASy (http://www.expasy.org/). The domains within the coding nucleotide sequence were forecasted by SMART (http://smart.embl-heidelberg.de/). Multiple protein sequence alignment was conducted using MEGA 5.0 and GeneDoc version X. The

Table 1
Primers used in this study.

Primer	Sequence (5′-3′)	PCR Object
ORFF	CCCACTTGTTCTGGGAAGCC	PCR screening
ORFR	AACTGAGTTAAGCGTCTTCCAGAAG	PCR screening
M13F	CGCCAGGGTTTTCCCAGTCACGAC	PCR screening
M13R	AGCGGATAACAATTTCACACAGGA	PCR screening
*Sp*BAG1F	GGCACTCACTAAGCTCAGGAAGCAG	qRT-PCR
*Sp*BAG1R	ACTAGTGCTTTCCGTCGCTGCCTGG	qRT-PCR
β-ActinF	GCGGCAGTGGTCATCTCCT	qRT-PCR
β-ActinR	GCCCTTCCTCACGCTATCCT	qRT-PCR
si*Sp*BAG1-1	GATCACTAATACGACTCACTATAGGGCAGGAAGCAGCTCCTTGCCGTTAATTT	RNAi
si*Sp*BAG1-2	CTAGTGATTATGCTGAGTGATATCCCGTCCTTCGTCGAGGAACGGCAATTAAA	RNAi
si*Sp*BAG1-3	AACAGGAAGCAGCTCCTTGCCGTTAATCCCTATAGTGAGTCGTATTAGTGATC	RNAi
si*Sp*BAG1-4	TTGTCCTTCGTCGAGGAACGGCAATTAGGGATATCACTCAGCATAATCACTAG	RNAi
siGFP1	GATCACTAATACGACTCACTATAGGGGGAGTTGTCCCAATTCTTGTT	RNAi
siGFP2	AACAAGAATTGGGACAACTCCCCCTATAGTGAGTCGTATTAGTGATC	RNAi
siGFP3	AAGGAGTTGTCCCAATTCTTGCCCTATAGTGAGTCGTATTA GTGATC	RNAi
siGFP4	GATCACTAATACGACTCACTATAGGGCAAGAATTGGGACAACTCCTT	RNAi
r*Sp*BAG1F	TGTTCCAGGGGCCCCTG**GGATCC**ATGGGTGACGAGGAGTACAGCATT	Recombinant expression
r*Sp*BAG1R	TCAGTCAGTCACGAT**GCGGCCGC**GGTGTAATTCAGCAGCAATTTG	Recombinant expression
VP466F	ATGTCTGCATCTTTAAT	WSSV copies
VP466R	TTATGACACAAACCTAT	WSSV copies
WSSV-RT1	TTGGTTTCATGCCCGAGATT	WSSV copies
WSSV-RT2	CCTTGGTCAGCCCCT TGA	WSSV copies

Note: Restriction enzyme sites are red.

phylogenetic tree was constructed using MEGA 5.0.

2.4. Tissue distribution and expression pattern analysis

Real-time quantitative PCR (qPCR) was used to assay the expression of *Sp*BAG1 in different tissues of healthy crabs and in hemocytes of WSSV-challenged crabs (at 0, 6, 24, 48, and 72 hpi). Total RNA was extracted and used as templates for cDNA synthesis using PrimeScript RT reagent Kit with gDNA Eraser (Takara, Dalian, China); the cDNA was used for amplifying the target gene (*Sp*BAG1) and the internal control (β-actin). The qPCR was carried out using the TransStart Top Green qPCR SuperMix (TransGen Biotech, Beijing, China) in LightCycler®480 (Roche, USA). The amplification procedure included a denaturation step of 95 °C for 30 s, and 40 cycles of 95 °C for 5 s, 60 °C for 20 s, followed by a melting curve analysis from 65 °C to 95 °C. Each sample was performed in three replicates. The PCR data were analyzed using the LightCycler 480 software (Roche, USA). The relative transcript level of *Sp*BAG1 was determined using the $2^{-\Delta\Delta Ct}$ algorithm. The data were subjected to one-way ANOVA analysis using Origin Pro8.0 followed by *t*-test, with $P < 0.05$ considered statistically significant.

2.5. Expression and purification of recombinant SpBAG1

The ORF of *Sp*BAG1 was amplified using specific primers (r*Sp*BAG1F and r*Sp*BAG1R, Table 1). After digestion with *Bam* HI and *Not* I, the PCR products were cloned into pGEX-6p-1 and transformed into *E. coli* (DE3) plysS competent cells (Novagen, Germany) for protein expression. After IPTG induction, the recombination protein expressed in the supernatant was purified as follows: harvested cells were resuspended in TBS (50 mM Tris, 100 mM NaCl, pH 8.0) and sonicated at 4 °C for 25 min with a sonicator (BILON-250Y) set at 3 s sonication and 4 s interval under 35% power. The cell lysates were then centrifuged at 10,000 rpm for 10 min at 4 °C to collect the supernatant (containing GST), and then ProteinIso® GST Resin (TransGen Biotech, Beijing, China) was added to purify the proteins.

2.6. Antibody preparation

The purified recombinant *Sp*BAG1 was used for antiserum preparation. First, five Balb/c mice were immunized four times in the first week with 100 μg of r*Sp*

BAG1 protein that was thoroughly mixed with Freund's Complete Adjuvant (MP Biomedicals, USA). Following this, 50 μg highly purified r*Sp*BAG1 thoroughly mixed with Freund's Incomplete Adjuvant (MP Biomedicals, USA) was injected two times once per week. A booster injection was administered a week later. Finally, mice sera were collected seven days after the final immunization and stored at −80 °C.

2.7. WSSV quantification and detection of apoptosis activity

A total of 24 mud crabs were randomly divided into two groups (including control and WSSV-challenged groups). A volume of 200 μL of WSSV (at 1×10^7 *cfu* mL^{-1}) was injected to each mud crab in the WSSV-challenged group and the same volume of PBS was injected to the control. At different time points (0, 24 and 48 h), the hemolymph from four crabs (per group) was collected and used for determination of the copies of WSSV and apoptosis rate. TaqMan real-time PCR was carried out to determine the copies of WSSV using the Premix Ex TaqTM (Probe qPCR) (TaKaRa, Dalian, China), labeled with the fluorescent dye 5-carboxyfluorescein (FAM) (5′-FAM-TGCTGCCGTCTCCAA-TAMRA-3′) and the primers WSSV-RT1 and WSSV-RT2 (Table 1). The copies of WSSV were quantified based on a standard curve for the WSSV quantification. A WSSV VP466 fragment was cloned into the pMD®19-T vector (TaKaRa, Dalian, China) with primers VP466F and VP466R (Table 1), and transformed into *E. coli*. The recombinant vector was purified and quantified using a UV spectroscopy. After a ten-fold dilution, the recombinant pMD®19-T vector was used for qPCR to generate the standard curves. Each reaction incorporated with 20 ng of mud crab DNA templates, 5 μL of 2 × Premix Ex TaqTM (Probe qPCR), 0.2 μL of each primer (10 μM), 0.15 μL of the probe (10 μM) and nuclease-free water to a total volume of 10 μL. The PCR was performed using LightCycler® 480 (Roche, USA) with the cycling conditions: initial denaturation at 94 °C for 3 min, 45 cycles at 95 °C for 5 s, 52 °C for 20 s and 72 °C for 20 s. Ct values were taken into the standard curve for calculation. The apoptosis rate of the hemocytes was evaluated using the FITC Annexin V Apoptosis Detection Kit I (BD Pharmingen™, USA) and mitochondrial membrane potential detection kit. Flow cytometry (AccuriTM C6 Plus, BD Biosciences, USA) and fluorescence microscopy were used to analyze the rate of apoptosis in the hemocytes. On the other hand, the Caspase-3 activity in hepatopancreas was determined using the Caspase-3 Activity Kit (Beyotime, Jiangsu, China). Results were expressed as μmol mg^{-1} protein. Each sample was tested in triplicates. The differences between different treatments were analyzed by *t*-test, with $P < 0.05$ considered statistically significant.

2.8. RNA interference of SpBAG1

RNA interference primers si*Sp*BAG1 A-D was designed according to the ORF sequence of *Sp*BAG1. MicroRNAs were synthesized using the *in vitro* Transcription T7 Kit (TaKaRa, Dalian, China). Next, 50 μg siRNA of *Sp*BAG1 (si*Sp*BAG1) was injected into each mud crab *via* the fourth leg, each about 30 g. In addition, the equivalent amount of siRNA targeting green fluorescent protein, GFP, (siGFP) was injected into the negative control group. At 48 h post siRNA injection, the hemocytes were collected and used for qPCR analysis by the specific primers (Q-*Sp*BAG1F and Q-*Sp*BAG1R). The efficiency of the RNA interference of *Sp*BAG1 based on internal control (β-actin) was determined.

2.9. Western blot analysis

After RNA interference, the protein levels of *Sp*BAG1 were determined by Western blot analysis. Hemocytes were collected and then treated with RIPA lysis buffer (Beyotime, Shanghai, China). The 12% SDS-PAGE was used to separate the proteins, which were then transferred onto nitrocellulose (NC) membranes. Mouse anti-BAG1 polyclonal antibodies (acts as a primary antibody) and horseradish peroxidase (HRP)-conjugated goat anti-mouse (Transgen Biotech., Beijing, China) (acts as a secondary antibody) were used to incubate the membranes. Tubulin was used as an internal reference protein. Antibody binding complexes were visualized with the BeyoECL Plus (Beyotime, Shanghai, China) on AI600 films (GE Healthcare).

2.10. WSSV challenge after SpBAG1 RNAi and the apoptosis rate of hemocytes

Following a successful knockdown of *Sp*BAG1 at 48 h post siRNA treatment, the mud crabs were then challenged with a 200 μL volume of WSSV (1×10^7 *cfu* mL^{-1}) for 48 h. The hemolymph from three crabs per group was collected, transferred into tubes, diluted with an anticoagulant solution for detecting the apoptosis rate of hemocytes and Caspase-3 activity. Detection of mitochondrial membrane potential was performed using the mitochondrial membrane potential detection kit (Beyoyime, Jiangsu, China). Each sample was tested in triplicates. The differences between different treatments were analyzed by *t*-test, with $P < 0.05$ considered statistically significant.

3. Results

3.1. Sequence and domain architecture of SpBAG1

The full-length cDNA sequence of *Sp*BAG1 (Fig. 1A) (1761 bp) contains an ORF of 630bp, encoding a deduced protein of 209 amino

```
GGATATTGTTTACACCGCGCGCCGAGTACCGCACTCCCACTTGTTCTGGGAAGCCTTCTA    1
ACTCTTGTCCCATCTGTATGTGGCTCTTTGGGAGGTTATTTAAGTCAAGTGCATCAAGGA   61
                  M  W  L  F  G  R  L  F  K  S  S  A  S  R     20
TGGGTGACGAGGAGTACAGCATTACGCTGTGCCACGGCACCTCCCGACACGATGTGCTGG  121
  M  G  D  E  E  Y  S  I  T  L  C  H  G  T  S  R  H  D  V  L   40
TGAAGGGCACCTTGACCTTGGAGGAGCTGTCTAGAACGATTGAGGAATTGACTGATGTGC  181
  V  K  G  T  L  T  L  E  E  L  S  R  T  I  E  E  L  T  D  V   60
TCCACAACAGCCAGAAAATCATTCACCGAGGGAAGACCCTGTCCCGGGGCGAGGCAACTC  241
  L  H  N  S  Q  K  I  I  H  R  G  K  T  L  S  R  G  E  A  T   80
TGGCATCATGTGGTGTGGGTCCCGGCGCCAAGTTGATGGTGCTAGGCAAGAAGCATGAAC  301
  L  A  S  C  G  V  G  P  G  A  K  L  M  V  L  G  K  K  H  E  100
ATGAGGACAACAGCATCAATTTTAAGGCTGTCCTAAAAATTGAGGAATCATGCAGCAAAG  361
  H  E  D  N  S  I  N  F  K  A  V  L  K  I  E  E  S  C  S  K  120
TAGAACGGCGCCTCAATGATGCCATTCCAGAGGTGGAAGGAATTTCACAAGGATACATGG  421
  V  E  R  R  L  N  D  A  I  P  E  V  E  G  I  S  Q  G  Y  M  140
ATCCCCAATTGTGTGGGGAGGCACTCACTAAGCTCAGGAAGCAGCTCCTTGCCGTTAATG  481
  D  P  Q  L  C  G  E  A  L  T  K  L  R  K  Q  L  L  A  V  N  160
AAGACTTCATGCGTCATCTGGAGCAGTTGGATGGTATTGATTTCCAGGAAACAGATGTTC  541
  E  D  F  M  R  H  L  E  Q  L  D  G  I  D  F  Q  E  T  D  V  180
GTGCCAGGCAGCGACGGAAAGCACTAGTGAAGAGAATCCAAGAGTTGATGGAACGGTGTG  601
  R  A  R  Q  R  R  K  A  L  V  K  R  I  Q  E  L  M  E  R  C  200
ACCGAGAACATGAACACATCAACAAATTGCTGCTGAATTACACCTAGTATTGGAGTGGCA  661
  D  R  E  H  E  H  I  N  K  L  L  L  N  Y  T  *              220
CCTTGTAGTTCAGCCTTCTGGAAGACGCTTAACTCAGTTTTCTAGTTTACACTCAGTGGT  721
GGGTTTTAATTAGCAGAGTGTGTGTAATATATTAATTTATACTTGTGCTATAAAAGAGTG  781
ACCTTGAGATTTAAAAGATGTGAGTGTGTTTTCAGCACATGGGAAGACTTGTTACACAGC  841
ATGCTGGCAGCTTGGTATGAGCAAAATCATAGATACTTAAACACTAGAGTGTTTTCACAT  901
GTACAATAACTGTTAATTAACTTTCAGAAGATGGGAAAATTACATTTTTTTTATCATTTT  961
```

(B)

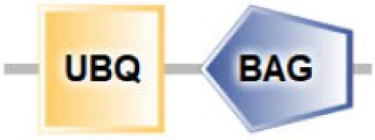

Fig. 1. Sequence analysis of *Sp*BAG1 (GenBank accession no. MK532474). (A) The nucleotide sequence and deduced amino acid sequence of *Sp*BAG1. The domain *Sp*BAG1 (*Sp*BAG1-interacting protein) was shadowed with a gray background. (B) The domain architecture of *Sp*BAG1 was predicted by SMART.

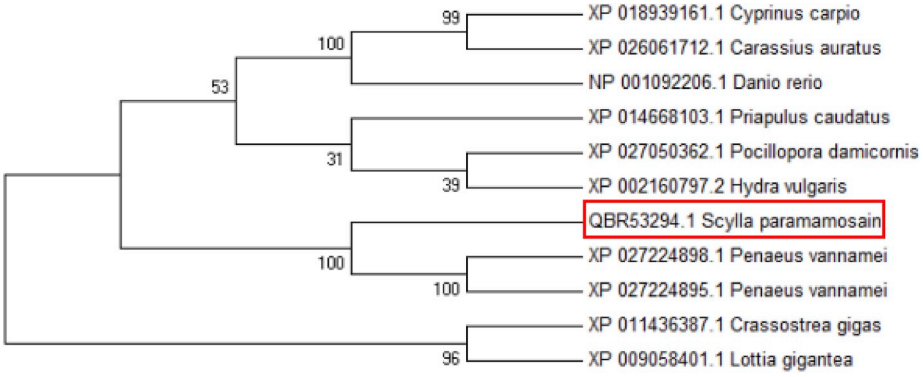

Fig. 2. Phylogenetic tree analysis of *Sp*BAG1 from different species. The *Sp*-BAG1 sequences of different animals were collected from GenBank and used to construct the neighbor-joining tree by MEGA 5.0 software. The animals included *Penaeus vannamei* (GenBank accession no. XP_027224898.1), *Penaeus vannamei* (XP_027224895.1), *Crassostrea gigas* (XP_011436387.1), *Lottia gigantea* (XP_009058401.1), *Cyprinus carpio* (XP_018939161.1), *Carassius auratus* (XP_026061712.1), *Pocillopora damicornis* (XP_027050362.1), *Danio rerio* (NP_001092206.1), *Hydra vulgaris* (XP_002160797.2), and *Priapulus caudatus* (XP_014668103.1). One thousand bootstraps were used in the phylogenetic tree.

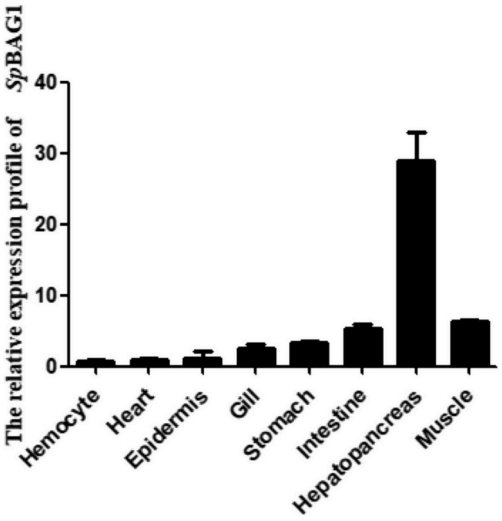

Fig. 3. The tissue distribution of *Sp*BAG1 in mud crab determined by RT-qPCR. The distribution analysis of *Sp*BAG1 in different tissues of mud crab by RT-qPCR. β-actin was used as the internal control. Total RNAs were extracted from tissues including hemocytes, heart, hepatopancreas, gills, stomach, epidermis, muscle and intestine. Significances were calculated by *t*-test.

acids (estimated molecular weight of 24.5kD). The putative *Sp*BAG1 protein is composed of an N-terminal ubiquitin-like (Ubl) domain (acids 21–91) and a BAG domain (acids 121–195) (Fig. 1B). The cDNA ORF sequence of *Sp*BAG1 has been deposited at NCBI GenBank under the accession number MK532474. A phylogenetic tree based on the amino acid sequences of *Sp*BAG1 and those from other species was constructed using MEGA 5.0. The results revealed that *Sp*BAG1 had an evolutional relationship with the *Penaeus vannamei* BAG1 and clustered with other arthropod BAG1 (Fig. 2), suggesting a certain degree of conservatism within invertebrate species.

3.2. Tissue distribution of SpBAG1 and expression profiles after WSSV challenge

Semi-quantitative RT-PCR was used to detect the distribution of *Sp*BAG1 in tissues at the mRNA level. *Sp*BAG1 could be detected in all tested tissues, including hemocytes, heart, hepatopancreas, gills, stomach, muscle, epidermis, and intestine, with the highest level in hepatopancreas (Fig. 3). The result demonstrated that *Sp*BAG1 ubiquitously distributed in mud crab tissues.

The expression profiles of *Sp*BAG1 in the hemocytes of mud crabs after challenge with WSSV at different point times were studied. The results revealed that *Sp*BAG1 was significantly increased at 6–24 hpi, but decreased from 48–72 hpi (Fig. 4). The results suggested that the expression of *Sp*BAG1 could be up-regulated in early stage, but down-regulated in the late stage of WSSV infection in the hemocytes of mud crab.

3.3. Expression and purification of recombinant protein pGEX-SpBAG1

The recombinant plasmid pGEX-*Sp*BAG1 correctly sequenced was transformed into host expressed bacteria of BL21. After IPTG induction, the recombinant protein pGEX-*Sp*BAG1 was mainly expressed in supernatant. SDS-PAGE electrophoresis was used to analyze the lysate, and the fusion protein band (Fig. 5A) was consistent with the predicted molecular weight (51.5kD). The induced pGEX-*Sp*BAG1 was purified with Proteinlso® GST Resin, and a relatively high concentration of purified protein was obtained (Fig. 5B) with a concentration of 3563.125 g/mL.

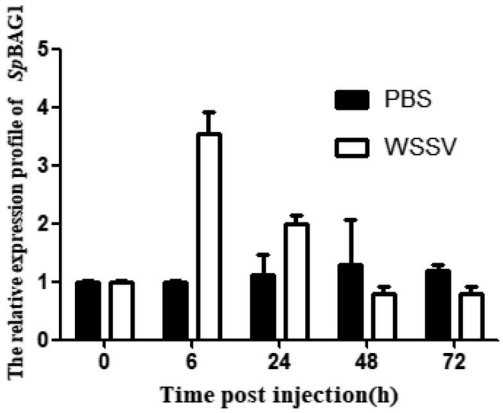

Fig. 4. The expression profiles of *Sp*BAG1 in mud crab after WSSV challenge. The expression of *Sp*BAG1 was investigated in the hemocytes of mud crab at 0,6, 24, 48, and 72 h post injection with WSSV (10^7 *cfu* mL^{-1}). The PBS-injected groups were used as the controls to remove the injury effect and β-actin as the internal control. Significances were calculated between the WSSV-challenged and the PBS-injected groups at the same time point by *t*-test. Statistical significance was indicated by asterisks (* $P < 0.05$).

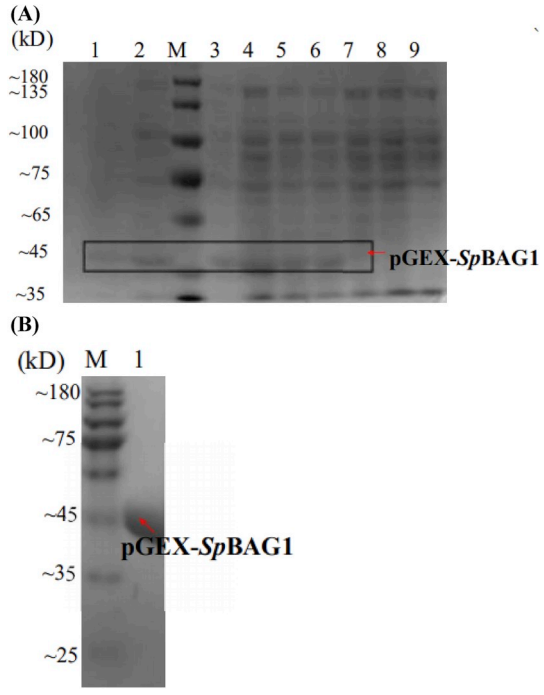

Fig. 5. Expression and purification of recombinant protein pGEX-*Sp*BAG1. (A) Lane A1 and A2: lysate precipitation induced by IPTG; Lane M: standard protein molecular weight; Lane A3, A4, A5 and A6: supernatant of lysate induced by IPTG; Lane A7, A8, A9: Empty Vector induced by IPTG. (B) Lanes B1: purified recombinant protein pGEX-*Sp*BAG1.

3.4. WSSV challenge induce apoptosis in the hemocytes of mud crab

The rate of apoptosis in hemocytes was detected at different time points (0, 24 and 48 h) after WSSV challenge. The results revealed that the apoptosis rate in the hemocytes of mud crab was up-regulated at 24 and 48 hpi during WSSV challenge (Fig. 6A). Furthermore, the activity of Caspase-3, which is a marker of apoptosis, and the copies of WSSV showed a significant increase (Fig. 6B and C). These results suggested the apoptosis of the hemocytes was activated with the increase of WSSV copies during the process of WSSV infection in mud crab.

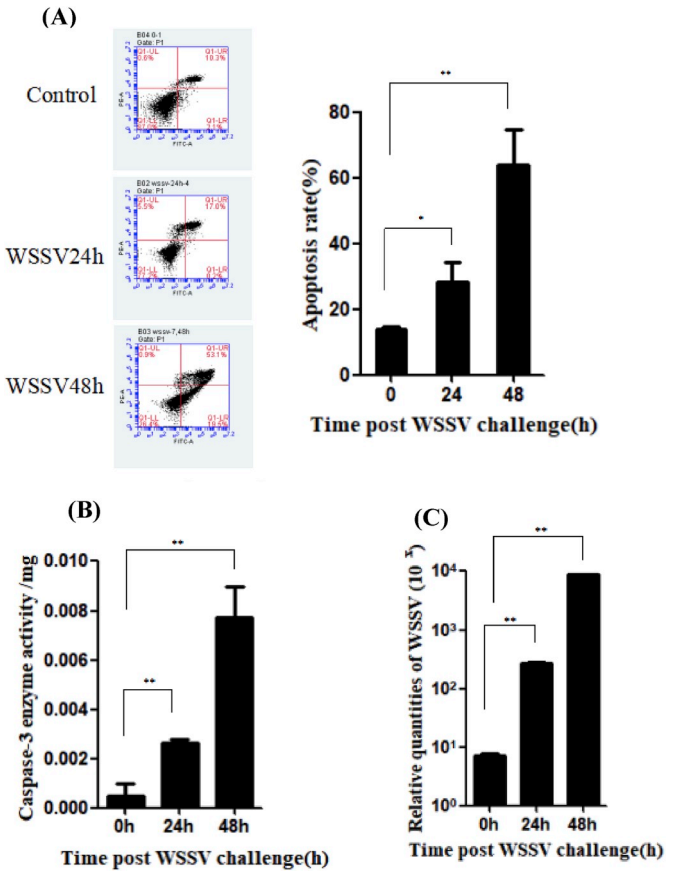

Fig. 6. The apoptotic rate, activities of caspase-3 enzyme, and the copies of WSSV in mud carb hemocytes after WSSV challenge (107 cfu mL^{-1}). (A), Hemocytes were collected at different time points (0 h, 24 and 48 h) during the WSSV challenge. Flow cytometry was used to analyze the challenge of apoptosis rate. (B), Detection of Caspase-3 enzyme activity. (C), The copies of WSSV.

3.5. WSSV replication and apoptosis rate of the hemocytes in SpBAG1 silenced mud crab

RNAi was performed to investigate the functions of *Sp*BAG1 in antiviral process in mud crab. Firstly, the knockdown efficiency of *Sp*BAG1 was determined using qRT-PCR and Western blot. The qRT-PCR results showed that the mRNA expression of *Sp*BAG1 was decreased by 78% (Fig. 7A). To ascertain the knockdown efficiency at the protein level, western blot analysis was also carried out after siRNA injection. The results showed that compared with the control, the injection of si*Sp*BAG1 attenuated *Sp*BAG1 protein expression in the hemocytes of mud crabs (Fig. 7B).

The results revealed that RNAi knock-down of *Sp*BAG1 significantly increased the apoptosis rate of hemocytes (the treatment group: 55%; the control group: 24%) (Fig. 8A) and significantly reduced the copies of WSSV (the treatment group: $10^{1.7}$ viral copies per ng muscle DNA; the control group: 10^{3} viral copies per ng muscle DNA) (Fig. 8C) after challenge with WSSV. Furthermore, the activity of Caspase-3 was found to be significantly increased (Fig. 8B), while such of mitochondrial membrane potential was significantly decreased (Fig. 8D and E) in the treatment group, compared to the controls ($P < 0.05$). The increased apoptosis rate and the activity of Caspase-3, the decreased mitochondrial membrane potential in the hemocytes in *Sp*BAG1 silenced mud crabs indicated that *Sp*BAG1 could promote WSSV replication by inhibiting the apoptosis of the hemocytes in mud crab during the viral infection.

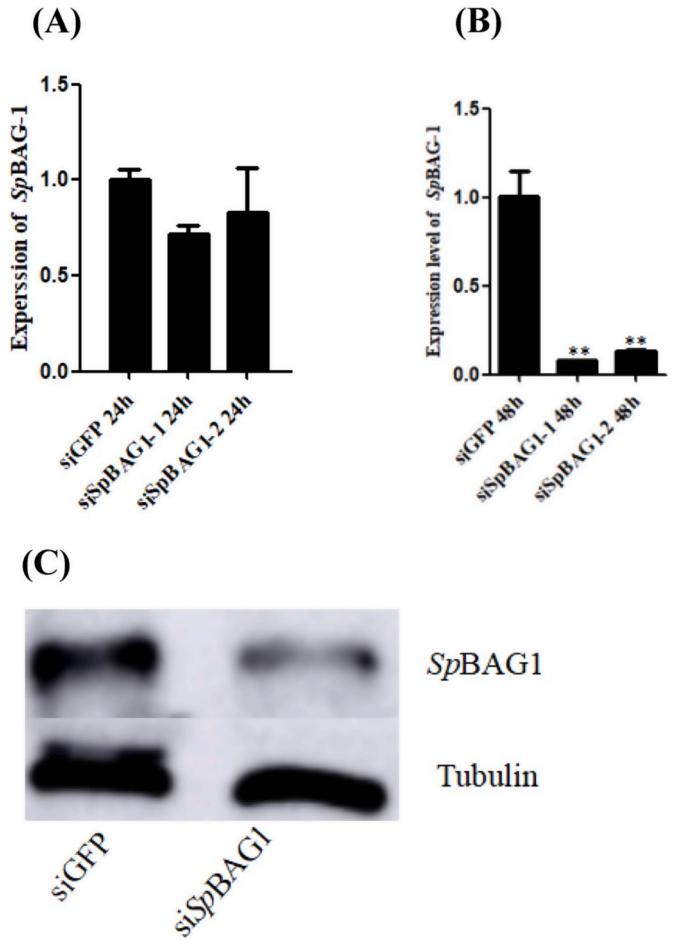

Fig. 7. The efficiency of *Sp*BAG1 RNAi in mud crab hemocytes. (A) and (B), The mRNA expression of *Sp*BAG1 at 24 h and 48 h in hemocytes after injection with si*Sp*BAG1. All data were normalized to siGFP treated samples and β-actin was used as an internal control. Data was shown as mean ± S.E. and significance was compared between the treatment and the control groups at the same time point. (C), Transcriptional level of *Sp*BAG1 after RNA interference of *Sp*BAG1. Asterisks indicated significant differences (* $P < 0.05$).

4. Discussions

Mud crab is one of the economically important crustacean species cultured in the southeastern coast of China [19]. Recently, the expansion of mud crab culture scales leads to the increase in a disease outbreak caused by both infectious pathogens (bacteria, fungus, and virus) and environmental factors. Of them, the virus-WSSV is a common pathogen caused huge economic losses in the mud crab culture industry. WSSV is a double-stranded DNA with double-layer envelope, short rod and no inclusion body [20], which belongs to *Nimaviridae whispovirus* [21]. WSSV is one of the most harmful pathogens to shrimp farming industry in the world, the annual economic losses caused by WSSV are more than 3 billion US dollars [22]. And there is also reported that mud crab is one of the natural carriers of WSSV with a natural carrier rate of 8.47%. The fact that WSSV can invade the mud crab through the oral route, and rapidly proliferate within mud crab to reach a certain amount that can cause diseases in the host [2]. The immune enhancers are considered to be mainly used in crustaceans, which enhance the phagocytosis, activation of phenoloxidase system, and activities of hemolymph antimicrobial lysis and immune-related enzymes [23–25]. However, the existing immune enhancers are not effective for protecting the host against all pathogens. Therefore, the exploration of more immune-related genes will provide more realistic guiding significance that is useful for the development and application of the

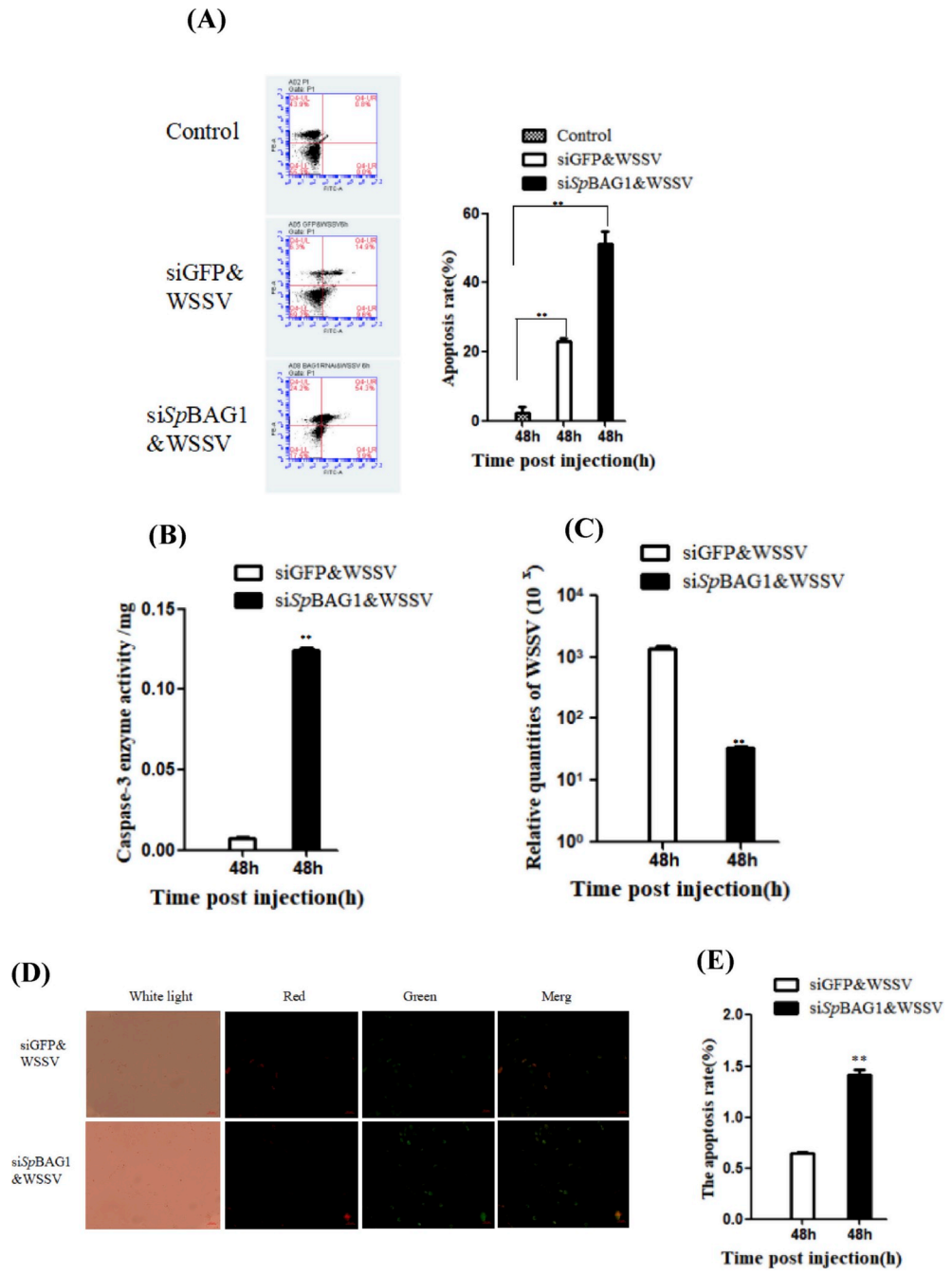

Fig. 8. The function of *Sp*BAG1 in the hemocytes in mud crab. The apoptosis rate (A), copies of WSSV (B), activities of Caspase-3 enzyme (C), and activities of mitochondrial membrane potential (D) and (E) in the hemocytes of mud crab after treatment with si*Sp*BAG1 followed by WSSV challenge.

immune enhancers in cultured animals [26]. Previous studies have shown that cell apoptosis is related to viral infection and considered to be an antiviral mechanism of insects and invertebrates. Cell apoptosis is a way that the organisms utilize to eliminate the viruses and control the spread of viruses within the cells, leading to maintaining the integrity of the organisms. For instance, influenza virus can induce apoptosis of human Hela cells, human monocytes, avian lymphocytes, and mouse macrophages [27–30]. In a recent study, it has been found a positive correlation between the number of apoptotic cells and the severity of WSSV infection in *Penaeus monodon*, suggesting that apoptosis may be the cause of death in WSSV-infected shrimps [31]. Results of the present study showed that the WSSV infection intensity is proportional to the apoptotic rate in the hemolymph of mud crab. These findings support a better understanding of the roles of apoptotic regulation in the antiviral reaction in the immune system of mud crab. Of which, the protein BAG1 acts as a multifunctional protein participate in the apoptotic process.

As a member of the BAG family, BAG1 was the first anti-apoptotic multifunctional protein screened from mammalian cytoplasm [32]. In several studies using the cancer cells from humans, the expression of BAG1 was overexpressed in breast cancer, gastric cancer, non-small cell cancer, cervical cancer, and prostate cancer [33–37]. Moreover, the effects of BAG1, including inhibiting cell apoptosis, promoting cell proliferation and regulating gene transfer, have been observed in humans and other mammals through its functional structure and action on the corresponding target cells [38,39]. The BAG1 protein is composed of a BAG region, an ubiquitin-like region, an amino acid residue repeat sequence and a nuclear localization signal. BAG1 (acts as a

multifunctional protein) can interact with many signal factors, including molecular chaperone Hsp70/Hsc70, Bcl-2, P53, nuclear hormone receptors, and retinoblastoma proteins [33,40], which is an effective biomarker for the occurrence and development of the tumors. However, little is known about BAG1 protein in invertebrates. In this study, we identified the BAG1 protein in mud crab, named *Sp*BAG1, which contained a putative BAG domain with three parallel alpha helixes and it shared high similarities with BAGs from other arthropods. Prediction of protein domain indicates that *Sp*BAG1 has typical BAG domain and ubiquitin-like domain, which is similar to found in mammals [41,42]. In mammals, BAG domain can interact directly with ATPasc domain of molecular chaperone Hsp70/Hsc70. It can also bind to specific proteins directly through N-terminal domain, and then regulate its binding to substrate protein [43]. However, the function of this protein in crab remains to be further studied.

WSSV infection experiment showed that, upon WSSV stimulation, the expression of BAG1 in the hemolymph of mud crab was up-regulated at (6–24 h), but down-regulated from 48 h to 72 h. The apoptotic rate of the cells was significantly increased. Up-regulation of *Sp*BAG1 expression at the early stage of infection can effectively inhibit the apoptosis of host cells and facilitate the replication of virus *in vivo*. In the late stage of infection, the host cells react to inhibit the replication of WSSV, thus inhibiting the expression of *Sp*BAG1, which promotes cell apoptosis to a certain extent, and can effectively eliminate the virus. The findings herein are consistent with the results of previous studies [44]. It has been reported that BAG1 was down-regulated (by 30% at 7 days) in the heart of mice after infection with Coxsackievirus B (CVB3) virus [45]. Different BAG1 subtypes, however, have shown different expression trends, for example, BAG1 subtype P32 was down-regulated (at 4 or 7 days), while BAG1 subtype P50 up-regulated (at 7 days) after CVB3 infection [45]. The occurrence of this phenomenon may be related to the viral proteins carried by the virus itself. Studies have shown that some viral infections can inhibit cell apoptosis, such as LMW5-HL of African swine fever virus (ASFV), BHRF1 of EB virus and other viral products are Bcl-2 analogues. BHRFl is a cytokine-induced inhibitor of apoptosis during the EB virus lysis cycle [46]. Actually, previous studies have confirmed the involvement of viral infection in the induction or inhibition of apoptosis in animals [47]. Viral infections usually lead to the expression of many genes that activates the protease and subsequently which induce the apoptosis. Previously, the up-regulation of BAG1 in the hippocampal neurons of herpes simplex virus (HSV)-infected African green monkey kidney has found to inhibit the apoptosis of neurons [48], but the regulation of BAG1 in the heart of CVB3-challenged mouse induced the apoptosis of BAG1 in the cytoplasm and nucleus. Thus, virus can induce or inhibit apoptosis of target cells. Our study data indicate that *Sp*BAG1 may be an important component promoting the WSSV infection through the apoptosis inhibition in the hemolymph in mud crabs.

In addition, RNAi knock-down of *Sp*BAG1 can significantly decrease the copies of WSSV and increase the apoptotic rate in mud crabs. Caspase-3 was more active than the control groups. The results of mitochondrial membrane potential test showed that the decrease of mitochondrial membrane potential was more obvious after knock-down *Sp*BAG1. The results of this experiment are contrary to those of previous experiments. In this process, the response of host cells may be dominant. The down-regulation of *Sp*BAG1 promotes cell apoptosis and inhibits virus replication. In addition, the changes of Caspase-3 activity and mitochondrial membrane potential suggest that the presence of *Sp*BAG1 may inhibit the release of apoptotic inducible factors in related apoptotic pathways, thereby inhibiting apoptosis. The results of this study are consistent with those of previous studies [49,50].

In conclusion, *Sp*BAG1 was the first identified from the mud crab, which may be an important component in the innate immune system of mud crab. *Sp*BAG1 was found to be up-regulated during the early infection stage with WSSV, suggesting that the WSSV infection can reduce up-regulate *Sp*BAG1 and inhibit apoptosis in mud crab. The silencing of *Sp*BAG1 significantly attenuated the copies of WSSV and elevated the apoptotic rate in mud crabs. The detected of Caspase-3 activation and mitochondrial membrane potential changes indicated that mitochondria activated Caspase-3 by releasing apoptosis-inducing factors and induce cell apoptosis. The findings from this study provide a better understanding of the functions of *Sp*BAG1 as an apoptotic inhibitor to promote virus infection in the immune defense of mud crabs during WSSV infection.

Acknowledgements

The work was supported by grants from National Natural Science Foundation of China (41876152, 31850410487, 31802341), Guangdong provincial project of Science and Technology (2017B020204003), the ‘Sail Plan’ Program for Outstanding Talents of Guangdong Province (14600605) and support from Department of Education of Guangdong Province (2017KCXTD014).

References

[1] S.P. Weng, Z.X. Guo, J.J. Sun, S.M. Chan, J.G. He, A reovirus disease in cultured mud crab, *Scylla serrata*, in southern China, J. Fish Dis. 30 (3) (2010) 133–139.
[2] X.S. Zhang, X.X. Tang, N.T. Tran, Y. Huang, Y. Gong, Y.L. Zhang, et al., Innate immune responses and metabolic alterations of mud crab (*Scylla paramamosain*) in response to *Vibrio parahaemolyticus* infection, Fish Shellfish Immunol. (2019), https://doi.org/10.1016/j.fsi.2019.01.011.
[3] C.W. Mariëlle, V. Hulten, R.W. Goldbach, J.M. Vlak, Three functionally diverged major white spot syndrome virus structural proteins evolved by gene duplication, J. Gen. Virol. 81 (10) (2000) 2525–2529.
[4] M.C. van Hulten, M. Westenberg, S.D. Goodall, J.M. Vlak, Identification of two major virion protein genes of white spot syndrome virus of shrimp, Virology 266 (2) (2000) 227–236.
[5] J.M. Tsai, H.C. Wang, J.H. Leu, H.H. Hsiao, A.H.J. Wang, G.H. Kou, et al., Genomic and proteomic analysis of thirty-nine structural proteins of shrimp white spot syndrome virus, J. Gen. Virol. 78 (20) (2004) 11360–11370.
[6] C. Huang, X. Zhang, Q. Lin, X. Xu, Z. Hu, C.L. Hew, Proteomic analysis of shrimp white spot syndrome viral proteins and characterization of a novel envelope protein VP466, Mol. Cell. Proteom. 1 (3) (2002) 223–231.
[7] D. De-Garzón, D. Saulnier, J. Garnier, C. Jouffrey, P. Bulet, E. Bachere, Crustacean immunity, J. Biol. Chem. 276 (50) (2001) 47070–47077.
[8] J.F.R. Kerr, A.H. Wyllie, A.R. Currie Apoptosis, A basic biological phenomenon with wide ranging implications in tissue kinetics, Br. J. Canc. 26 (4) (1972) 239–257.
[9] R. Paus, T. Rosenbach, N. Haas, B.M. Czarnetzki, Patterns of cell death: the significance of apoptosis for dermatology, Exp. Dermatol. 2 (1) (1993) 3–11.
[10] A. Bergmann, J. Agapite, H. Steller, Mechanisms and control of programmed cell death in invertebrates, Oncogene 17 (25) (1998) 3215–3223.
[11] R.J. Clem, L.K. Miller, Control of programmed cell death by the baculovirus genes p35 and iap, Mol. Cell. Biol. 14 (8) (1994) 5212–5222.
[12] R.J. Clem, L.K. Miller, Apoptosis reduces both the in vitro replication and the in vivo infectivity of a baculovirus, J. Virol. 67 (7) (1993) 3730–3738.
[13] A.H. Koyama, A. Adachi, H. Irie, Physiological significance of apoptosis during animal virus infection, Int. Rev. Immunol. 22 (5–6) (2003) 341–359.
[14] E.V. Doukhanina, S. Chen, E. van der Zalm, A. Godzik, J. Reed, M.B. Dickman, Identification and functional characterization of the BAG protein family in *Arabidopsis thaliana*, J. Biol. Chem. 281 (27) (2006) 18793–18801.
[15] L. Brive, S. Takayama, K. Briknarová, S. Homma, S.K. Ishida, J.C. Reed, et al., The carboxyl-terminal lobe of Hsc70 ATPase domain is sufficient for binding to BAG1, Biochem. Biophys. Res. Commun. 289 (5) (2001) 1099–10105.
[16] R.I. Pennell, C. Lamb, Programmed cell death in plants, Plant Cell 9 (7) (1997) 1157–1168.
[17] I. Yao, T. Ohtsuka, H. Kawabe, Y. Matsuura, Y. Takai, Y. Hata, Association of membrane-associated guanylate kinase-interacting protein-1 with Raf-1, Biochem. Biophys. Res. Commun. 270 (2) (2000) 538–542.
[18] J. Song, M. Takeda, R.I. Morimoto, Bag1–Hsp70 mediates a physiological stress signalling pathway that regulates Raf-1/ERK and cell growth, Nat. Cell Biol. 3 (3) (2001) 276–282.
[19] T.T. Kong, Y. Gong, Y. Liu, X.B. Wen, T.T. Ngoc, J.A. Jude, et al., Scavenger receptor B promotes bacteria clearance by enhancing phagocytosis and attenuates white spot syndrome virus proliferation in, *Scylla paramamosian*, Fish Shellfish Immunol. 78 (2018) 79–90.
[20] C. Reville, J. Al-Beik, D. M-Meola, Z.K. Xu, M. Goldsmith, W. Rand, et al., White spot syndrome virus in frozen shrimp sold at Massachusetts supermarkets, J. Shellfish Res. 24 (2005) 285–290.
[21] M.A. Mayo, A summary of taxonomic changes recently approved by ICTV, Arch. Virol. 147 (8) (2002) 1655–1656.
[22] P.S. Leung, L.T. Tran, Predicting shrimp disease occurrence: artificial neural networks vs. logistic regression, Aquaculture 187 (1) (2000) 35–49.
[23] J. Ortuño, M.A. Esteban, J. Meseguer, High dietary intake of α-tocopherol acetate enhances the non-specific immune response of gilthead seabream (*Sparus aurata* L), Arch. Virol. 10 (4) (2000) 293–307.

[24] P.K. Sahoo, S.C. Mukherjee, Effect of dietary β-1,3 glucan on immune responses and disease resistance of healthy and aflatoxin B1-induced immune-compromised rohu (*Labeo rohita* Hamilton), Fish Shellfish Immunol. 11 (8) (2001) 683–695.
[25] S.I. Jang, M.J. Marsden, Y.G. Kim, M.S. Choi, C.J. Secombes, The effect of glycyrrhizin on rainbow trout, *Oncorhynchus mykiss* (Walbaum), leucocyte responses, J. Fish Dis. 18 (4) (2010) 307–315.
[26] D.P. Anderson, Immunostimulants, adjuvants and vaccine carriers in fish: application to aquaculture, Annu. Rev. Fish Dis. 2 (1992) 281–307.
[27] T. Takizawa, S. Matsukawa, Y. Higuchi, S. Nakamura, Y. Nakanishi, R. Fukuda, Induction of programmed cell death (apoptosis) by influenza virus infection in tissue culture cells, J. Gen. Virol. 74 (11) (1993) 2347–2355.
[28] H. Fesq, M. Bacher, M. Nain, D. Gemsa, Programmed cell death (apoptosis) in human monocytes infected by influenza a virus, Immunobiology 190 (1) (1994) 175–182.
[29] V.S. Hinshaw, C.W. Olsen, N. Dy-Sissoko, D. Evans, Apoptosis: a mechanism of cell killing by influenza A and B viruses, J. Virol. 68 (6) (1994) 3667–3673.
[30] J. Zhou, H.K. Law, C.Y. Cheung, I.H. Ng, J.S. Peiris, Y.L. Lau, Functional tumor necrosis factor-related apoptosis-inducing ligand production by avian influenza virus-infected macrophages, J. Infect. Dis. 193 (7) (2006) 945–953.
[31] C.B. Granja, L.F. Aranguren, O.M. Vidal, L. Aragón, M. Salazar, Does hyperthermia increase apoptosis in white spot syndrome virus (WSSV)-infected *Litopenaeus vannamei*? Dis. Aquat. Org. 54 (1) (2003) 73–78.
[32] S. Takayama, T. Sato, S. Krajewski, K. Kochel, S. Irie, J.A. Millan, et al., Cloning and functional analysis of BAG-1: a novel Bcl-2-binding protein with anti-cell death activity, Cell 80 (2) (1995) 279–284.
[33] S.C. Tang, BAG-1, an anti-apoptotic tumour marker, IUBMB Life 53 (2) (2002) 99–105.
[34] R. Kikuchi, T. Noguchi, S. Takeno, Y. Funada, H. Moriyama, Y. Uchida, Nuclear BAG-1 expression reflects malignant potential in colorectal carcinomas, Br. J. Canc. 87 (10) (2002) 1136–1139.
[35] D.A. Tennant, R.V. Durán, E. Gottlieb, Targeting metabolic transformation for cancer therapy, Nat. Rev. Cancer 10 (4) (2010) 267–277.
[36] X. Yang, Y. Hao, A. Ferenczy, S.C. Tang, A. Pater, Overexpression of anti-apoptotic gene BAG-1 in human cervical cancer, Exp. Cell Res. 247 (1) (1999) 200–207.
[37] H. Klocker, H. Rogatsch, Z. Culig, G. Bartsch, N. Knezevic, S. Liubov, et al., Expression of the androgen receptor coactivator Bag1 is upregulated in prostate cancer, Eur. Urol. Suppl. 2 (1) (2003) 84-84.
[38] A. Bardelli, P. Longati, D. Albero, S. Goruppi, C. Schneider, C. Ponzetto, et al., HGF receptor associates with the anti-apoptotic protein BAG-1 and prevents cell death, EMBO J. 15 (22) (1996) 6205–6212.
[39] R. Liu, Interaction of BAG-1 with retinoic acid receptor and its inhibition of retinoic acid-induced apoptosis in cancer cells, J. Biol. Chem. 273 (27) (1998) 16985–16992.
[40] E.A. Nollen, J.F. Brunsting, J. Song, H.H. Kampinga, R.I. Morimoto, Bag1 functions *in vivo* as a negative regulator of Hsp70 chaperone activity, Mol. Cell. Biol. 20 (3) (2000) 1083–1088.
[41] K. Briknarová, S. Takayama, L. Brive, M.L. Havert, D.A. Knee, J. Velasco, et al., Structural analysis of BAG1 cochaperone and its interactions with Hsc70 heat shock protein, Nat. Struct. Mol. Biol. 8 (4) (2001) 349–352.
[42] S. Fang, L. Li, B. Cui, S. Men, Y. Shen, X. Yang, Structural insight into plant programmed cell death mediated by BAG proteins in *Arabidopsis thaliana*, Acta Crystallogr. D Biol. Crystallogr. 69 (6) (2013) 934–945.
[43] H.M. Beere, D.R. Green, Stress management-heat shock protein-70 and the regulation of apoptosis, Trends Cell Biol. 11 (1) (2001) 6–10.
[44] H.G. Wang, T. Miyashita, S. Takayama, T. Sato, T. Torigoe, S. Krajewski, et al., Apoptosis regulation by interaction of Bcl-2 protein and Raf-1 kinase, Oncogene 9 (9) (1994) 2751–2756.
[45] T. Peng, T. Sadusky, Y. Li, G.R. Coulton, H. Zhang, L.C. Archard, Altered expression of Bag-1 in coxsackievirus B3 infected mouse heart, Cardiovasc. Res. 50 (1) (2001) 46–55.
[46] M. Kawanishi, Epstein-Barr virus BHRF1 protein protects intestine 407 epithelial cells from apoptosis induced by tumor necrosis factor alpha and anti-Fas antibody, J. Virol. 71 (4) (1997) 3319–3322.
[47] M. Sumikoshi, K. Hashimoto, Y. Kawasaki, H. Sakuma, T. Suzutani, H. Suzuki, et al., Human influenza virus infection and apoptosis induction in human vascular endothelial cells, J. Med. Virol. 80 (6) (2008) 1072–1078.
[48] D. Perkins, E.F.R. Pereira, L. Aurelian, The herpes simplex virus type 2 R1 protein kinase (ICP10 PK) functions as a dominant regulator of apoptosis in hippocampal neurons involving activation of the ERK survival pathway and upregulation of the antiapoptotic protein Bag-1, J. Virol. 77 (2) (2003) 1292–1305.
[49] H.G. Wang, T. Miyashita, S. Takayama, T. Sato, T. Torigoe, S. Krajewski, et al., Apoptosis regulation by interaction of Bcl-2 protein and Raf-1 kinase, Oncogene 9 (9) (1994) 2751–2756.
[50] F. Yang, W.L. Zhou, A.L. Liu, H.L. Qin, S.M. Lee, Y.T. Wang, et al., The protective effect of 3-Deoxysappanchalcone on *in vitro* influenza virus-induced apoptosis and inflammation, Planta Med. 78 (10) (2012) 968–973.